IJMMM International Journal of Minerals, Metallurgy and Materials 矿物冶金与材料学报（英文版）

Bonding of compound casted Ti/Al bimetal by heat treatment

M. Fadaeinia and Ramin Raiszadeh

Cite this article as:
M. Fadaeinia and Ramin Raiszadeh, Bonding of compound casted Ti/Al bimetal by heat treatment, *Int. J. Miner. Metall. Mater.*, 28(2021), No. 9, pp. 1515-1524. https://doi.org/10.1007/s12613-020-2107-z

View the article online at SpringerLink or IJMMM Webpage.

International Journal of Minerals, Metallurgy and Materials
Volume 28, Number 9, September 2021, Page 1515
https://doi.org/10.1007/s12613-020-2107-z

Bonding of compound casted Ti/Al bimetal by heat treatment

M. Fadaeinia and Ramin Raiszadeh

Department of Metallurgy and Materials Science, School of Engineering, Shahid Bahonar University of Kerman, Kerman 7616913439, Iran
(Received: 20 December 2019; revised: 22 May 2020; accepted: 25 May 2020)

Abstract: The formation mechanism of the bonding between compound cast Al/Ti bimetal during a heat treatment regime was investigated. Commercially pure Al was cast and melt on a Ti bar in a steel tube, followed by heat treatment on the compound cast Ti/Al bimetal for different periods of time once the Al melt was solidified. No bonding was observed between the two metals after the initial casting, which can be attributed to the presence of oxide films on the liquid Al and solid Ti alloys and the trapped atmosphere between them. The effect of these layers in preventing the formation of bonding was eliminated after heat treating the cast part at ~973 K (~700°C) for at least 15 min, and the metals started to bond with each other. A detailed description of this bonding mechanism is presented in this paper.

Keywords: compound casting; titanium/aluminium bimetal; bonding

1. Introduction

At present, compound casting is commonly used to join two similar or dissimilar metals [1]. In this method, a liquid metal is poured around another metal, which is in the solid state. The liquid metal diffuses into the solid one, thus forming solid solutions and/or intermetallic phases. Such a diffusion reaction causes the two metals to bond to each other. This method has been used to join many similar or dissimilar metals, such as steel/Al [2], Cu/Al [3], Al/Al [4], steel/Cu [5], and Al/Mg [6].

In the case of reactive metals, such as Al and Ti, the oxide layer that forms on the liquid and/or solid metal might prevent the formation of seamless bonding between the two metals. In particular, Zare *et al.* [1] suggested that the shear stress exerted upon the oxide layer during the pouring of the liquid metal might tear it apart and remove it from the surface of the liquid metal, thus facilitating the formation of a seamless bonding. However, many researchers have reported the formation of a defective bonding due to the presence of such layers [7–9].

Recently, Yousefi and Doostmohammadi [9], who investigated the formation mechanism of an Al–$TiAl_3$ *in situ* composite fabricated by a compound casting method, observed that heat treating the compound cast Al/Ti bimetal part at temperatures ranging from 973 to 1173 K (700°C–900°C) for 180 min eliminated the deleterious effect of the oxide layers and caused the formation of the $TiAl_3$ intermetallic. They offered two possible explanations for this observation: (1) the breakage of the oxide layers during the heat treatment process due to the difference between the thermal expansion coefficients of the oxide and the substrate metal; (2) the reduction of the TiO_2 by Al.

Yousefi and Doostmohammadi [9] also showed that heat treatment is a simple, cost-effective, and efficient method for improving the bonding between two metals in compound cast parts, compared to other methods used for the same purpose [10–12]. Therefore, the commercial application of this method entails understanding the mechanism of the elimination of the deleterious effect of the oxide layers during the heat treatment. In the current study, an experimental method originally used by this research team [13–16] to study the behavior of bifilm defects in different Al alloys was adopted to study the effect of heat treatment on the bonding mechanism between Ti and Al in a compound casting process.

2. Experimental

A commercially pure Ti bar (99.8wt%, 50 mm in height and 19.5 mm in diameter) was inserted in a seamless extruded steel tube (made for gas industries). The steel tube (length and internal diameter of 100 mm and 20 mm, respectively) was welded upright on a steel plate. The upper base of the Ti bar was polished to 9 μm before it was inserted into the

Corresponding author: Ramin Raiszadeh E-mail: rraiszadeh@uk.ac.ir, rraiszadeh@yahoo.com

steel tube. Commercially pure Al alloy (99.8wt%) was then melted in a resistance-heated furnace to a super heat of 973 K (700°C) and poured in the steel tube, after the tube was pre-heated to about 573 K (300°C) in the furnace. The steel tube was allowed to cool down in the ambient temperature.

For the heat treatment of the Ti/Al bimetal in the steel tube, the tube was first transferred to an electric furnace, which was set at 973 K (700°C). On the basis of a few preliminary experiments, this temperature was chosen in such a way that the reaction between the two metals took place at a reasonable rate (i.e., as fast as possible, but not so fast that some observations would be lost). The tube remained in the furnace for certain periods of time (between 5 and 180 min) and was then removed from the furnace. The Al bar melted in the steel tube as it remained in the furnace for approximately 9.5 min (measured in a separate experiment using a K-type thermocouple inserted at the center of the Al bar). When the Al bar was melted in the tube, the oxide layer around the top of the Al melt was removed using a sharp tool beneath the surface of the melt. This was done to remove the oxide separating the melt from the steel tube.

Upon solidification, the steel tube was cut in two halves, and the Ti and Al bars were removed from the tube. If the bars were bonded to each other, they were separated using a Zwick 1484 tensile testing machine at a strain rate of 1 $mm \cdot min^{-1}$. The surfaces of the Ti and Al bars, which were in contact with each other during the experiment, were then photographed and examined using optical microscopy and Camscan scanning electron microscope (SEM) fitted with an Oxford Inca energy-dispersive X-ray spectroscopy (EDS) for microanalysis. The phases that were present at different parts of the samples were identified using an X'pert X-ray diffraction (XRD) device. To limit the area subjected to the X-ray, the surface of the sample, except the area of interest, was covered by a thick fiberglass duct tape. In the experiment with a heat treatment time of 180 min in which the two bars were bonded with each other, the bars were cut perpendicular to the bonded interface using electrical discharge machining. Then, the cross section of the bonded alloys was studied by SEM, EDS, and an image analysis technique (ImageJ 1.52J software).

3. Results

Fig. 1 shows the change in the temperature of the Al bar while undergoing heating inside the furnace. The Al bar started to melt after about 9.5 min, and the melting was completed after about 17.5 min.

3.1. After the casting

The photographs of the bases of the Ti and Al bars after casting and heat treatment are shown in Fig. 2. Fig. 2(a) shows the photographs of the bases of the Ti and Al bars after

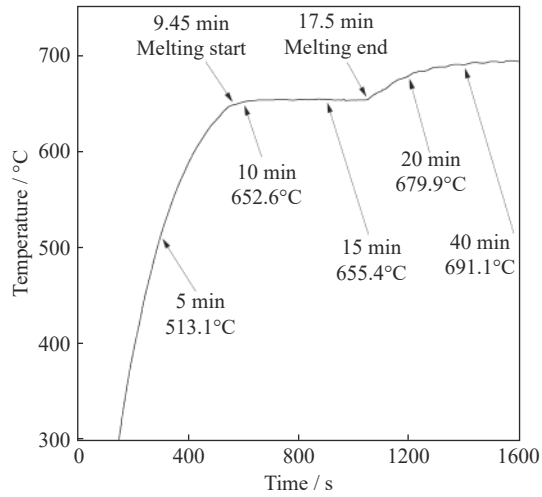

Fig. 1. Change in the temperature of the Al bar during the heat treatment.

the casting. The surface of the Ti bar showed changes in color in some areas. However, the only element detected by both XRD and EDS spectra (not presented here for brevity) was Ti. Furthermore, many depressions can be observed on the surface of the Al bar.

A secondary electron (SE) SEM micrograph obtained from this surface is shown in Fig. 3. As can be seen, the uneven surface of the base of the Al bar was covered by a layer of alumina. An interesting feature observed occasionally in the SEM micrographs obtained from this surface (one of which was denoted by an arrow in Fig. 3) was the exudation of liquid Al through this surface. A higher magnification of such an exudation is shown in Fig. 4. This Al melt exudation through the oxide layer in a commercially pure Al melt has been observed previously by this research team [14].

3.2. After 5 min of heat treatment

The temperature of the Al bar reached about 513°C (still in the solid state) after 5 min of heat treatment (Fig. 1). Fig. 2(b) presents the photograph of the base of the Ti and Al bars after 5 min of heat treatment. As can be seen, the change in the color of the Ti base intensified. Furthermore, the XRD spectra obtained from points P1 and P2 in this figure, also shown in Fig. 5, revealed the presence of the AlN, TiO, TiO_2, and $TiAl_3$ phases in these points. In this figure, and also Figs. 8, 10, and 13, the long unidentified peak at 28.712° was from the silicon in the duct tape, which covered the surface area of the sample except the area of interest. A semiquantitative analysis carried out using the X'pert highScore Plus software, based on the scale factor and the reference intensity ratio of the accepted phases, revealed that the mass fraction of TiO was higher at point P1 than that at point P2, whereas the mass fractions of the other phases were almost the same. This comparison implies that the darkening of the surface of the Ti bar can be attributed to the oxidation of the metal.

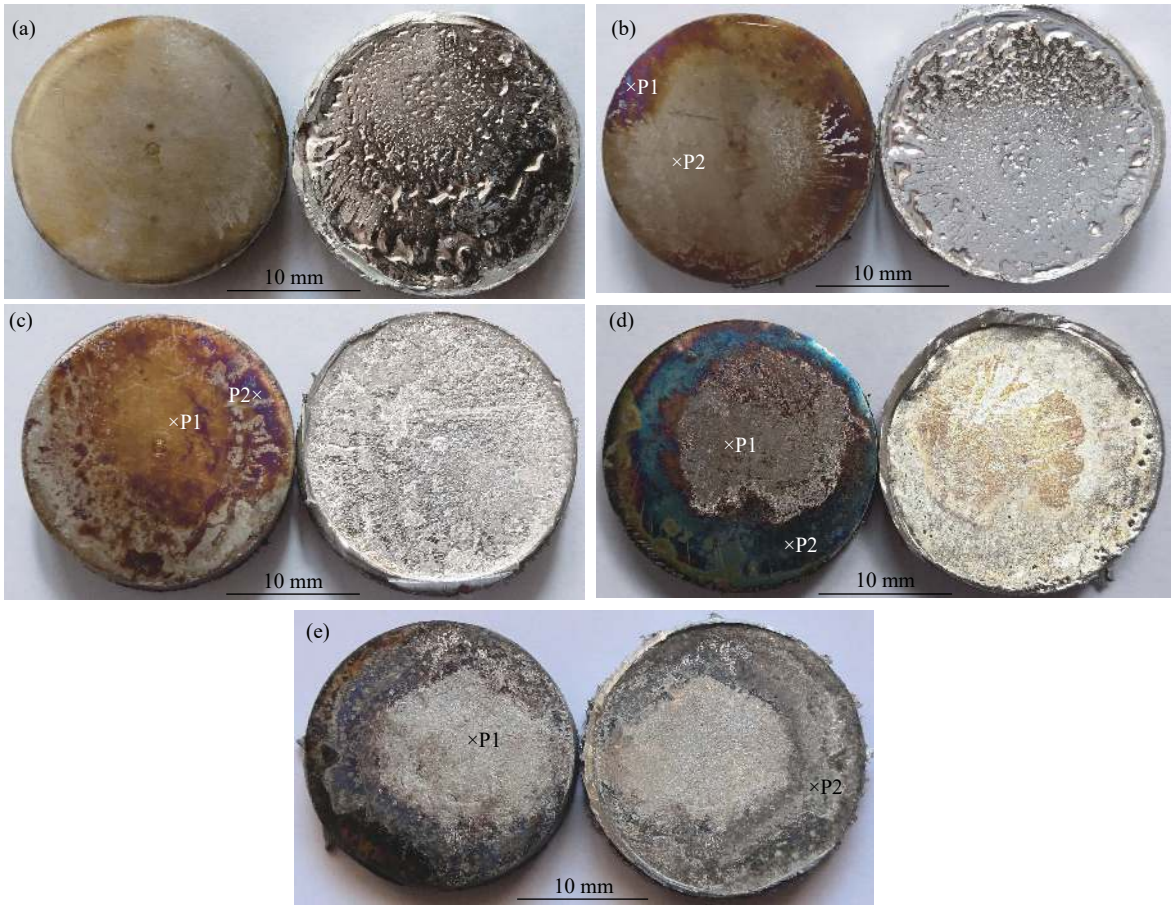

Fig. 2. Photographs of the bases of the Ti (left) and Al (right) bars after (a) 0, (b) 5, (c) 10, (d) 15, and (e) 40 min of heat treatment.

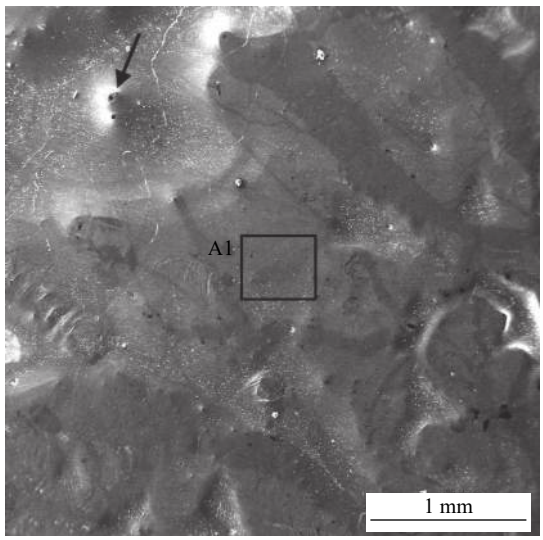

Fig. 3. SEM micrograph (SE) of the base of the Al bar after casting. The contents of elements at area A1 were measured to be 99wt% Al and 1wt% O.

Meanwhile, the figure also shows that some parts of the Al bar adhered to the Ti bar. This is evident in the secondary electron SEM (Fig. 6) and the corresponding EDS spectra (Fig. 7) taken from the surface of the Ti bar. These two figures also confirmed the formation of a titanium aluminide phase (point P3) at this heat treatment time.

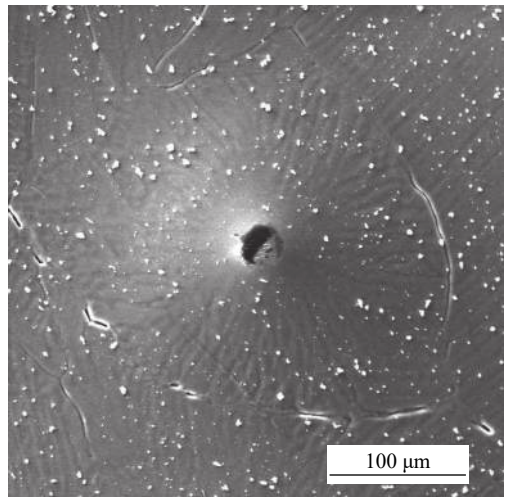

Fig. 4. Higher magnification SEM image of the Al bar base after casting, which shows the exudation of the Al melt through the oxide layer.

3.3. After 10 min of heat treatment

Fig. 2(c) shows the photographs of the bases of the Ti and

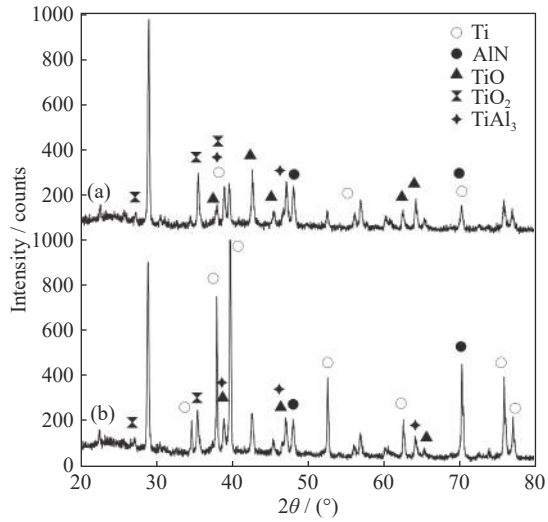

Fig. 5. XRD spectra obtained from points (a) P1 and (b) P2 in Fig. 2(b).

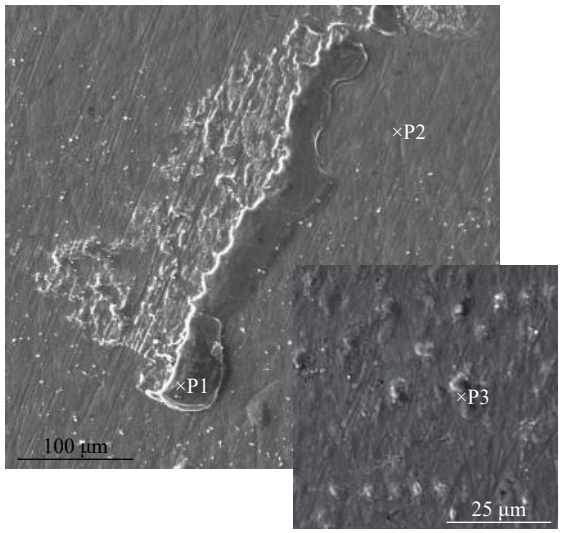

Fig. 6. SEM micrographs (SE) of the surface of the Ti bar after 5 min of heat treatment. Inset shows the magnifying image of the matrix.

Al bars after 10 min of heat treatment, when the temperature of the Al bar reached 652°C. As can be seen, the depressions disappeared from the surface of the Al bar. The XRD spectra obtained from points P1 and P2 in Fig. 2(c), shown in Fig. 8, revealed that no TiO_2 phase can be found in the sample. The titanium oxide phases detected at points P1 and P2 were TiO and Ti_2O. Fig. 8 also reveals the presence of Al_2O_3 at point P2. The AlN and $TiAl_3$ phases were also present at both points.

The formation of titanium aluminide was evident in the secondary electron SEM micrograph obtained from the base of the Ti bar at this heat treatment time, as shown in Fig. 9. As shown in the EDS spectra obtained from points P1 and P2 in this figure, the lighter phase contained about 13wt% Al and 87wt% Ti, whereas the darker phase contained 100wt%

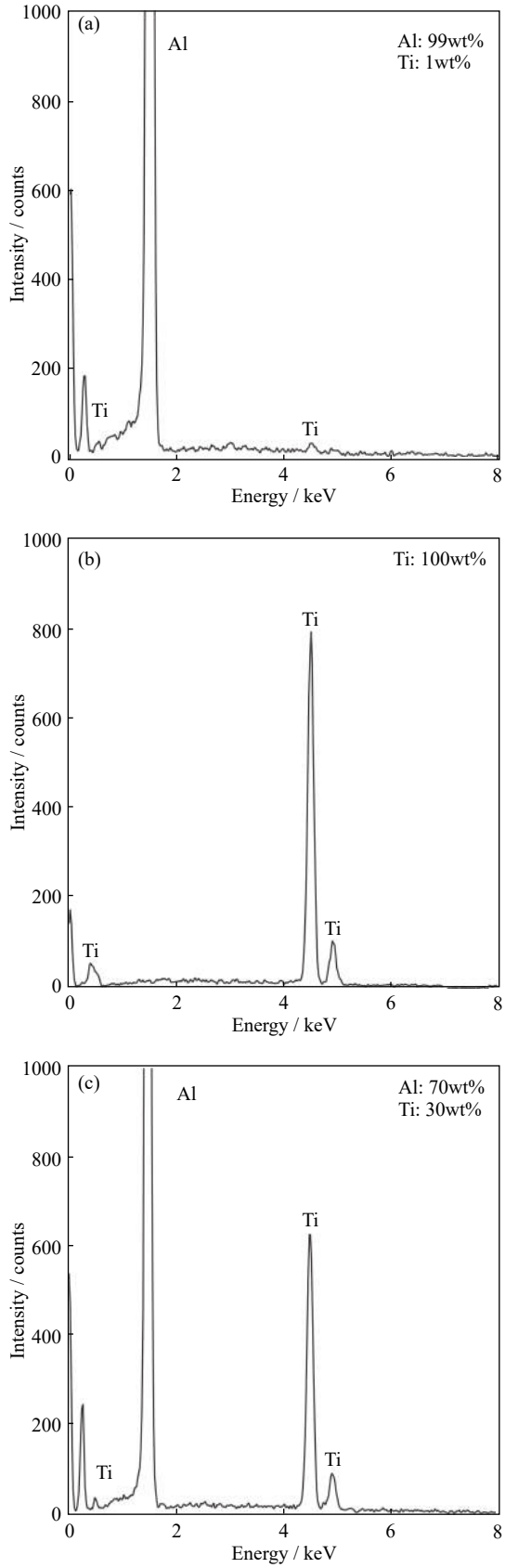

Fig. 7. EDS analyses obtained from points (a) P1, (b) P2, and (c) P3 in Fig. 6.

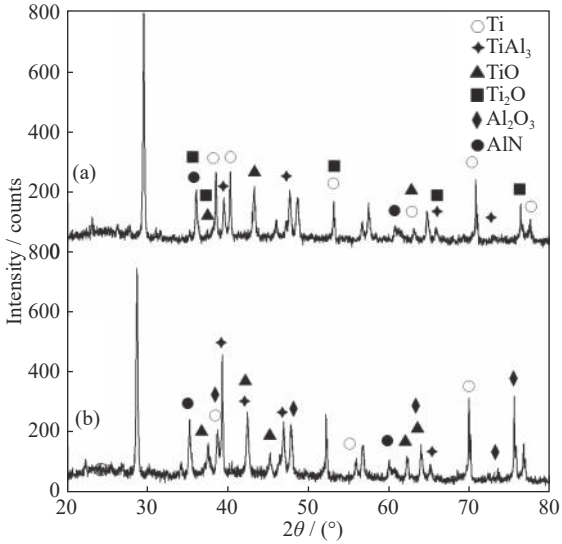

Fig. 8. XRD spectra obtained from points (a) P1 and (b) P2 in Fig. 2(c).

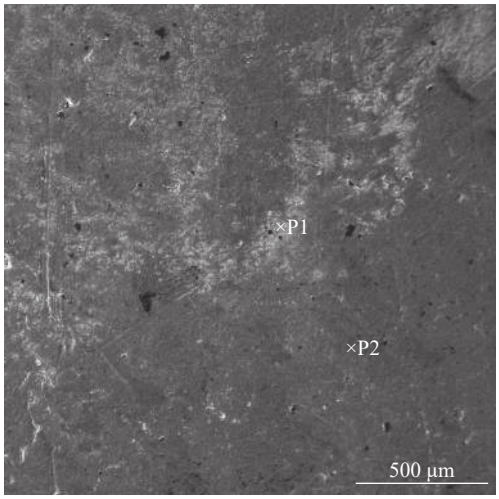

Fig. 9. SEM micrograph (SE) of the base of the Ti bar after 10 min of heat treatment. The contents of Al at points P1 and P2 in this figure were measured to be 13wt% and 0wt%, respectively.

Ti. Furthermore, no oxygen peak was found in these two EDS spectra.

3.4. After 15 min of heat treatment

The change in the color of the Ti base was significant when the sample was heat treated for 15 min (Fig. 2(d)). As shown in Fig. 1, about 70% of the Al bar melted at this heat treatment time. A big portion of the central part of the Ti and Al bars were bonded to each other, although these were then peeled off during the removal of the bars from the tube. This central part, according to the XRD spectrum obtained from point P1 in Fig. 2(d) shown in Fig. 10(a), contained the Ti_2N, AlN, and TiAl phases. The outer part of the base of the bar

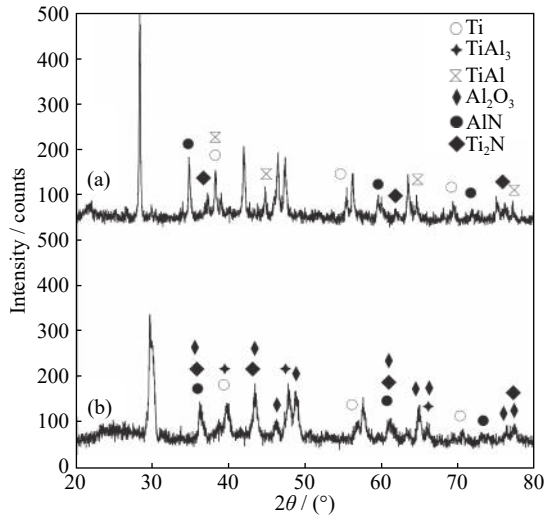

Fig. 10. XRD spectra obtained from points (a) P1 and (b) P2 in Fig. 2(d).

became dark blue in color. Meanwhile, the XRD spectrum obtained from point P2 (shown in Fig. 10(b)) revealed the presence of Al_2O_3, $TiAl_3$, Ti_2N, and AlN in this part of the Ti bar surface. However, no titanium oxide phase was observed on the surface of the Ti bar at this heat treatment time.

Fig. 11 shows a back scattered (BSE) SEM micrograph obtained from the surface of the Ti bar after undergoing 15 min of heat treatment. This micrograph was obtained from point P2 in Fig. 2(d). Three distinct phases can be observed in this micrograph (Fig. 11): pure Al bonded to the surface of the Ti bar (point P1), a titanium aluminide phase (identified by the XRD spectra shown in Fig. 10 to be $TiAl_3$) (point P2), and the Ti substrate (point P3). The identities of these phases were confirmed through the EDS spectra shown in Fig. 12. Point P2 also contained about 12wt% oxygen, which implied the presence of Al_2O_3 at this point. The presence of alumina at the outer area of the surface of the Ti bar at this heat treat-

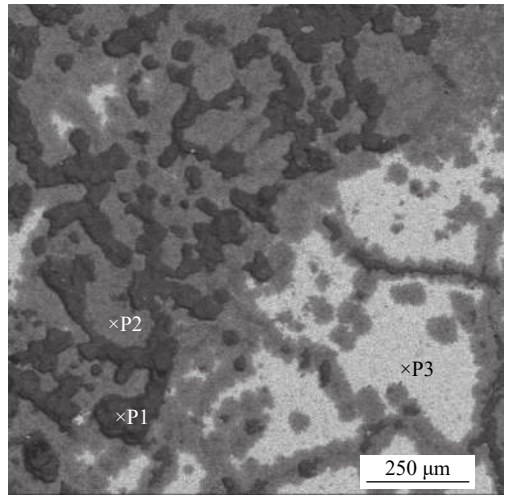

Fig. 11. SEM micrograph (BSE) from the base of the Ti bar after 15 min of heat treatment.

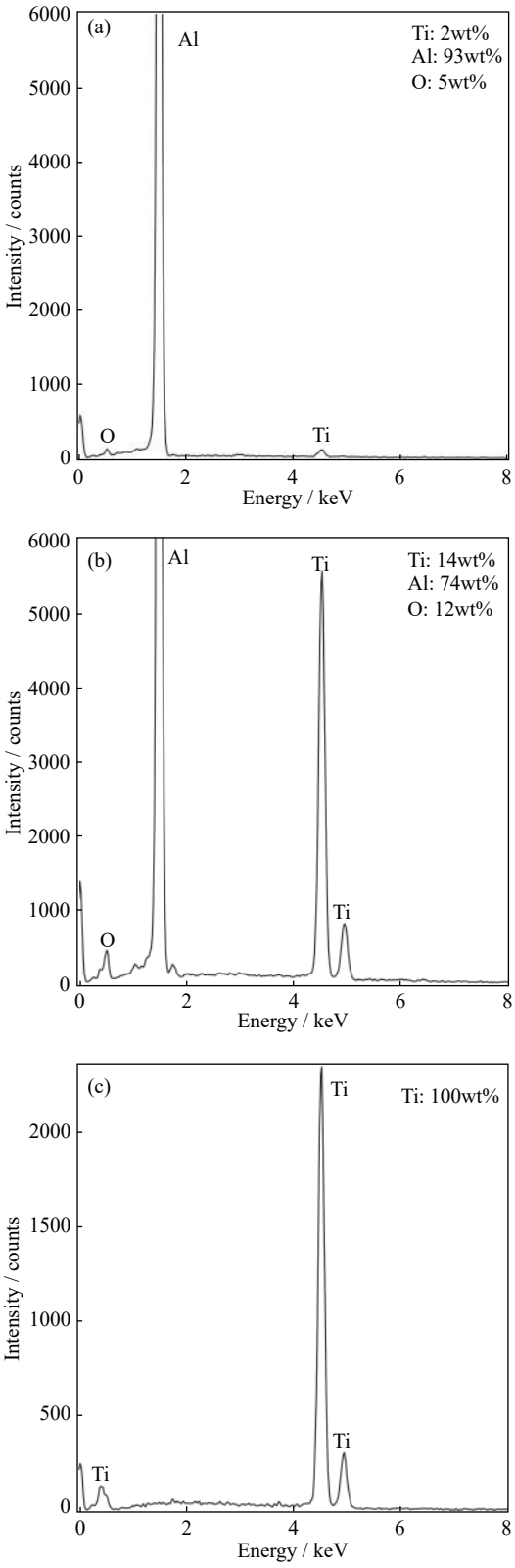

Fig. 12. EDS analyses from points (a) P1, (b) P2, and (c) P3 in Fig. 11.

ment time was also confirmed by the XRD spectrum presented in Fig. 10.

3.5. Heat treatment after 40 min and beyond

The Al and Ti bars bonded to each other at the center when the bars were heat treated for 40 min (Fig. 2(e)). The XRD spectra obtained from points P1 and P2 in Fig. 2(e) are presented in Fig. 13. These spectra revealed the presence of AlN, $TiAl_3$, TiAl, and Al at point P1 and AlN, $TiAl_3$, and Al at point P2. No oxide phase was observed in the XRD spectra obtained from the samples from this heat treatment time onwards.

A BSE SEM micrograph, obtained from the vertical cross section of the bonded bars after 180 min of heat treatment, is shown in Fig. 14. The figure shows how the Ti bar dissolved in the liquid Al and formed titanium aluminide phases. This diffusion then caused the formation of a seamless bond between the two alloys. The EDS spectra obtained from

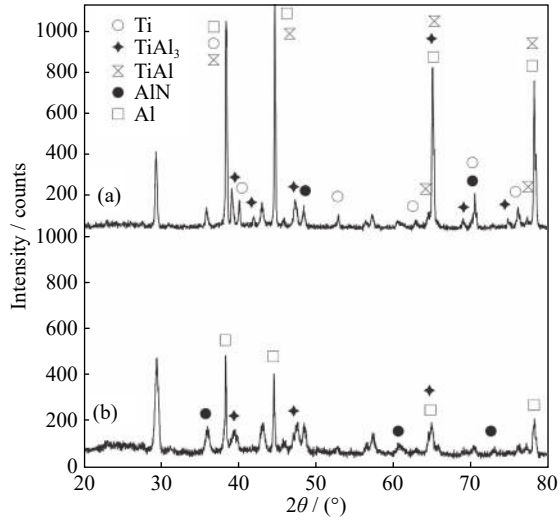

Fig. 13. XRD spectra obtained from points (a) P1 and (b) P2 in Fig. 2(e).

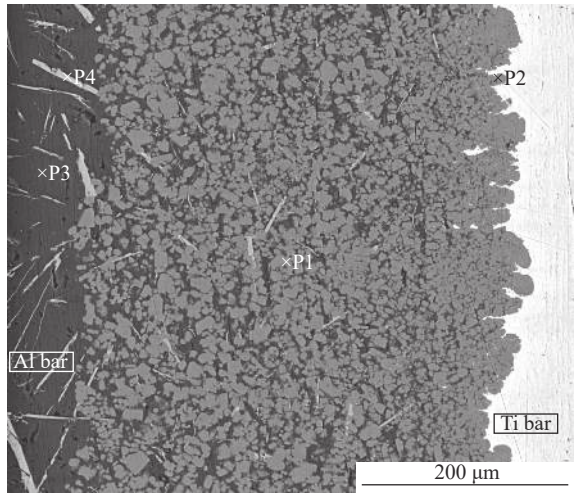

Fig. 14. SEM micrograph (BSE) from the vertical cross section of the interface between the Ti and Al bars after 180 min of heat treatment.

points P1 to P4 in Fig. 14, as shown in Fig. 15, revealed the identities of the phases observed in this microstructure. The contents of elements at the intermetallic phase formed between the Ti and Al bar (Point P1) were measured to be 61wt% Al and 36wt% Ti. The mass ratio of Ti to Al at this point (about 0.59) was the same as that in the $TiAl_3$ phase (0.59). In comparison, at point P2, the contents of elements were measured to be 22wt% Al and 78wt% Ti, with a Ti/Al mass ratio of about 3.54. The formation of the TiAl phase (with a Ti/Al mass ratio of 1.78) likely occurred at this point. At point P3, the contents of elements were measured to be about 99.1wt% Al and 0.9wt% Ti, indicating an almost saturated solution of Ti in Al. The results of the image analysis performed in Fig. 14 are presented in Fig. 16, which shows that the fraction of the microstructure occupied by the $TiAl_3$ particles decreased from the Ti bar toward the Al bar.

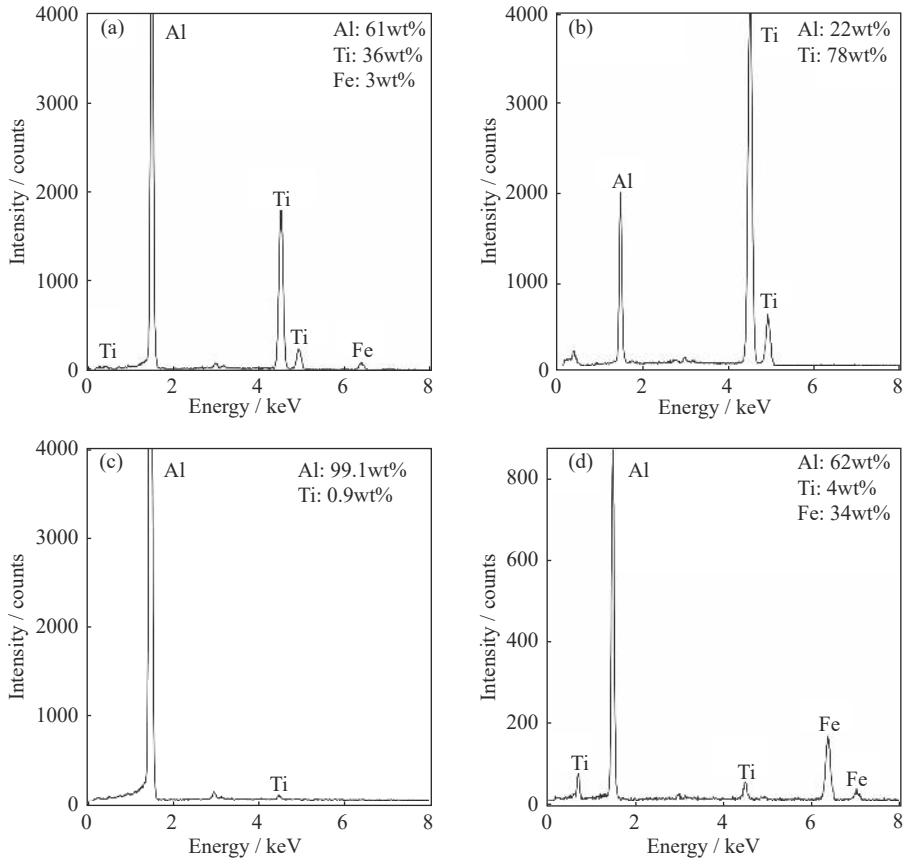

Fig. 15. EDS spectra obtained from points (a) P1, (b) P2, (c) P3, and (d) P4 in Fig. 14.

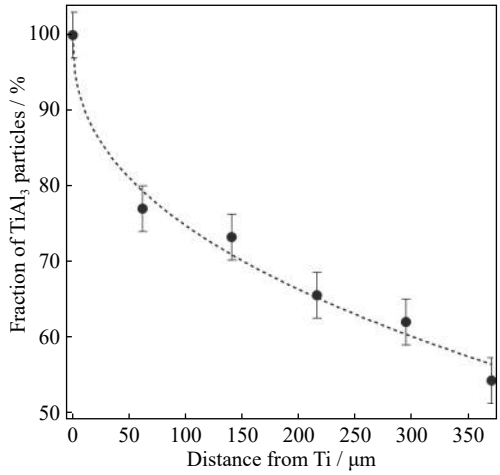

Fig. 16. Fraction of the microstructure occupied by the $TiAl_3$ particles.

Several β Fe-rich phases have also been observed in the Al bar (i.e., point P4 in Fig. 14) as well as in the interface zone. The formation of this phase was the result of the dissolution of Fe from the steel tube into the Al melt during the long heat treatment time of 180 min.

4. Discussion

The Gibbs free energy values ($\Delta G^{\ominus}$) of formation of the titanium oxides are highly negative (−850 and −744 kJ/mol oxygen for TiO and TiO_2, respectively, at 700°C [17]). Therefore, the surface of the Ti bar was covered by an extremely thin layer of titanium oxide (5–10 nm thick [18]) before the casting. No titanium oxide was found in the XRD or EDS spectra, which were obtained from the surface of the Ti bar after the casting, due to the extreme thinness of the oxide

layer. During the casting, this thin but solid Ti oxide came into contact with the solid Al_2O_3 layer, which covered the aluminum melt. The contact of the two unwetted solid oxide layers caused some air to get trapped between them, and these pockets of trapped air can be clearly seen in the photographs obtained from the surface of the Al bars after the casting (Fig. 2(a)) and after 5 min of heat treatment (Fig. 2(b)).

The thickness of the titanium oxide layer increased during the first 5 min of the heat treatment, and the peaks for TiO and TiO_2 phases appeared in the XRD spectra (Fig. 5). This observation is in accordance with that reported by Pouilleau *et al.* [19], who observed that the first oxide formed on a pure Ti substrate consisted of three layers: a TiO layer adjacent to the metallic Ti substrate, a TiO_2 layer that was in contact with the environment, and a TiO_x layer in between. They stated that the composition of TiO_x varied continuously through the thickness of the oxide layer so it was not detected by XRD.

Moreover, the oxygen required for this oxidation reaction was provided by the trapped atmosphere between the two bars. The volume of the depressions observed on the base of the Al bar gradually decreased as the gases in the trapped atmosphere were consumed (compare Figs. 2(a), 2(b), and 2(c)).

The presence of the $TiAl_3$ phase in the XRD spectra obtained from the surface of the Ti bar, which was subjected to the heat treatment for 5 min (Fig. 5), revealed that the liquid Al and Ti came into contact with each other at certain points. Meanwhile, Fig. 4 illustrates that liquid Al penetrated through the Al_2O_3 layer at some points and entered into the trapped atmosphere. This opportunity could be provided for the liquid Al when some cracks form on the oxide layer due to the following reasons:

(1) the turbulent pouring of the Al melt [20];

(2) the solidification and remelting of an initial thin layer of Al on the Al/Ti interface;

(3) the difference between the thermal expansion coefficients of Al and Al_2O_3;

(4) the relatively large increase in volume of the Al while it is melting.

The exuded liquid Al reacted with the oxygen of the trapped atmosphere to form more alumina. When the oxygen of the trapped atmosphere was consumed, both Ti and Al started to react with the nitrogen found in the trapped atmosphere to form AlN and Ti_2N, respectively. The former phase was present in all the XRD spectra obtained from the surface of the Ti bars in this research, except the one from the Ti bar after casting (with no heat treatment). This implies that such a phase is a relatively thick and predominant layer. The latter phase was observed only on the surface of the Ti bar heat treated for 15 min (Fig. 10).

Despite the presence of the atmosphere between the titanium oxide and alumina layers, it is highly likely that these two layers were in contact with each other at certain points at the moment of casting. However, the consumption of O and N found in the trapped atmosphere would force the oxide layers to come into contact with each other in more areas. The exudation of fresh liquid Al at these contact points (especially after the consumption of the gases within the trapped atmosphere) caused the titanium oxide to be reduced by the Al melt according to Eq. (1) [9]. The gradual reduction of titanium oxides by Al is evident in the XRD spectra (Table 1).

$$3TiO_2 + 4Al = 2Al_2O_3 + 3Ti,\quad \Delta G^{\ominus} = -506.3\ J\cdot mol^{-1} \text{ at } 1000\ K \tag{1}$$

Table 1. Oxides observed in the XRD spectra obtained from the Ti surface at different heat treatment times

Heat treatment time / min	TiO_2	TiO	Ti_2O	Al_2O_3
5	√	√		
10		√	√	
15				√
40				

Table 1 implies that Eq. (1) occurred gradually during the heat treatment through the following steps:

$$3TiO_2 + 2Al = 3TiO + Al_2O_3 \tag{2}$$

$$6TiO + 2Al = 3Ti_2O + Al_2O_3 \tag{3}$$

$$3Ti_2O + 2Al = 6Ti + Al_2O_3 \tag{4}$$

Fig. 2(d) shows that the Al and Ti bars started to bond to each other after about 15 min of heat treatment. Aryafar *et al.* [21] reported that two A356 Al bars bonded to each other when the two following conditions were met: (1) the almost complete consumption of the atmosphere trapped between the two bars and (2) the transformation at the contact areas of the two bars. Amirinejhad *et al.* [15] and Shafaei and Raiszadeh [20] also showed that the rate of bonding formation depends on the rates of both conditions and their sequence. The same was observed in the current experiments. The significant bonding between the two metals occurred only as a result of two conditions: (1) after at least a significant portion of the gases trapped between them were consumed by the reactions with both Al and Ti; (2) when the surfaces of the bars were forced into contact with each other. Thereafter, the dissolution of Ti into Al and the formation of titanium aluminides caused the two metals to bond with each other.

Moreover, Ti dissolved in Al in places where the two metals came into contact with each other. $TiAl_3$ particles nucleated and grew at these locations. As shown in Fig. 16, the fraction of the microstructure occupied by the $TiAl_3$ particles was higher adjacent to the Ti bar, and that it gradually decreased away from this interface. This observation indicated that the $TiAl_3$ particles that nucleated and grew at the interface between Al and Ti broke away from the interface and were pushed away into the liquid Al. This explanation is in accordance with the mechanism proposed by Harach and Vecchio [22], who attributed the fracture of the $TiAl_3$

particles from the interface to the stresses resulting from the difference between the Ti and $TiAl_3$ densities. Such a breakaway phenomenon disintegrated the oxide and nitride layers, thus providing seamless contact between the liquid Al and the Ti bar.

Therefore, the mechanism of bonding formation between Ti and Al during a heat treatment regime after a compound casting process can be summarized as follows (Fig. 17):

(1) the entrapment of some gases (predominantly air) between the liquid Al (which is covered by an extremely thin layer of Al_2O_3) and the Ti bar (which is covered by an extremely thin layer of TiO_2) (Fig. 17(a));

(2) the consumption of O and N of the trapped atmosphere by the liquid Al, which is exuded through the Al_2O_3 layer and the solid Ti (Fig. 17(b));

(3) the reduction of TiO_2 by the Al melt (exuded through the Al_2O_3 layer) to TiO and then to Ti_2O (Fig. 17(c)) at the locations where the two oxide layers are forced to come into contact with each other;

(4) the reduction of the Ti oxides to Ti and the consumption of the remaining N of the trapped atmosphere by the liquid Al and the solid Ti (Fig. 17(d));

(5) the dissolution of Ti in the liquid Al to form a saturated solution at some locations wherein the two metals come into contact with each other (Fig. 17(e));

(6) the nucleation and growth of $TiAl_3$ (and/or other titanium aluminides) from the saturated solution on the solid Ti bar as well as the fracture and expulsion of the $TiAl_3$ particles from the nucleation site due to stresses and rupture of the oxide and nitride layers, thus allowing seamless contact between the liquid Al and solid Ti and the resumption of the reaction between Ti and Al (Fig. 17(f)).

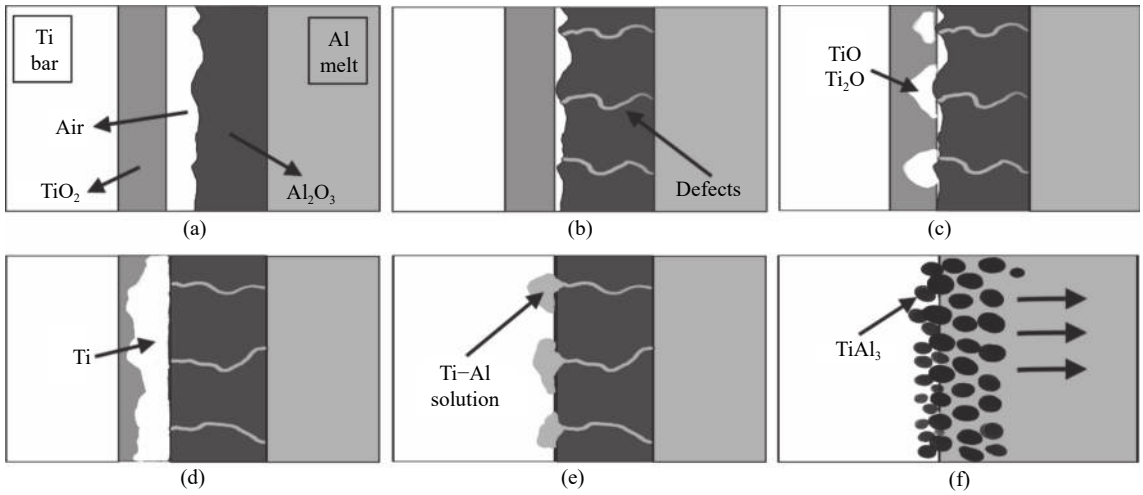

Fig. 17. Mechanism of bonding formation between the Ti and Al bars during heat treatment: (a) entrapment of air between two oxide layers during pouring; (b) consumption of O and N of the entrapped air by Al and Ti through defects formed in the oxides; (c) reduction of TiO_2 to TiO and Ti_2O and (d) finally to Ti by Al melt; (e) dissolution of Ti in the Al melt; (f) nucleation, growth, and expulsion of $TiAl_3$, which caused the oxide and nitride layers to rupture completely.

5. Conclusions

The mechanism of bonding formation between compound cast Al and Ti bimetal subjected to a heat treatment regime was investigated, and the following results were obtained:

(1) The two metals did not show signs of bonding after the compound casting, and this can be attributed to the presence of oxide layers on both metals.

(2) The pockets of air trapped between the two metals during the casting prevented the two oxide layers to come into complete contact with each other. The N and O contents of these air pockets were gradually consumed by the Al melt, which was exuded through the alumina layer, and the solid Ti, and the two oxide layers gradually came into better contact with each other.

(3) The TiO_2 layer that covered the Ti bar was reduced by the Al melt at some discrete areas. This reduction facilitated the contact between the liquid Al and the solid Ti. The Ti dissolved in the Al melt, and the $TiAl_3$ particles nucleated and grew on the Ti bar.

(4) The bonding between the two metals started after about 15 min of heat treatment. From this point onward, the ability of the oxide and nitride layers to prevent the bonding formation was eliminated. The elimination of these layers can be attributed to the expulsion of the $TiAl_3$ particles from the nucleation sites on the Ti bar into the Al melt which, in turn, caused the layers to disintegrate.

References

[1] G.R. Zare, M. Divandari, and H. Arabi, Investigation on inter-

face of Al/Cu couples in compound casting, *Mater. Sci. Technol.*, 29(2013), No. 2, p. 190.
[2] J. Pan, M. Yoshida, G. Sasaki, H. Fukunaga, H. Fujimura, and M. Matsuura, Ultrasonic insert casting of aluminum alloy, *Scripta Mater.*, 43(2000), No. 2, p. 155.
[3] M. Divandari and A.R.V. Golpayegani, Study of Al/Cu rich phases formed in A356 alloy by inserting Cu wire in pattern in LFC process, *Mater. Des.*, 30(2009), No. 8, p. 3279.
[4] M. Scanlan, D.J. Browne, and A. Bates, New casting route to novel functionally gradient light alloys, *Mater. Sci. Eng. A*, 413-414(2005), p. 66.
[5] J.S. Ho, C.B. Lin, and C.H. Liu, Effect of continuous cooling heat treatment on interface characteristics of S45C/copper compound casting, *J. Mater. Sci.*, 39(2004), No. 7, p. 2473.
[6] E. Hajjari, M. Divandari, S.H. Razavi, S.M. Emami, T. Homma, and S. Kamado, Dissimilar joining of Al/Mg light metals by compound casting process, *J. Mater. Sci.*, 46(2011), No. 20, p. 6491.
[7] K.J.M. Papis, B. Hallstedt, J.F. Löffler, and P.J. Uggowitzer, Interface formation in aluminium–aluminium compound casting, *Acta Mater.*, 56(2008), No. 13, p. 3036.
[8] T.M. Wang, C.H. Liang, Z.N. Chen, Y.P. Zheng, H.J. Kang, and W. Wang, Development of an 8090/3003 bimetal slab using a modified direct-chill casting process, *J. Mater. Process. Technol.*, 214(2014), No. 9, p. 1806.
[9] M. Yousefi and H. Doostmohammadi, Microstructure characterization and formation mechanism of functionally graded Al–$TiAl_3$ *insitu* composite by liquid–solid interaction, *J. Alloys Compd.*, 766(2018), p. 721.
[10] S.G. Robertson, I.M. Ritchie, and D.M. Druskovich, A kinetic and electrochemical study of the zincate immersion process for aluminium, *J. Appl. Electrochem.*, 25(1995), No. 7, p. 659.
[11] M. Rübner, M. Günzl, C. Körner, and R.F. Singer, Aluminium–aluminium compound fabrication by high pressure die casting, *Mater. Sci. Eng. A*, 528(2011), No. 22-23, p. 7024.
[12] C. Koerner, M. Schwankl, and D. Himmler, Aluminum–aluminum compound castings by electroless deposited zinc layers, *J. Mater. Process. Technol.*, 214(2014), No. 5, p. 1094.
[13] F.N. Bakhtiarani and R. Raiszadeh, The behaviour of double oxide film defects in Al–4.5wt% Mg melt, *J. Mater. Sci.*, 46(2011), No. 5, p. 1305.
[14] F.N. Bakhtiarani and R. Raiszadeh, Healing of double-oxide film defects in commercial purity aluminum melt, *Metall. Mater. Trans. B*, 42(2011), No. 2, p. 331.
[15] S. Amirinejhad, R. Raiszadeh, and H. Doostmohammadi, Study of double oxide film defect behaviour in liquid Al–Mg alloys, *Int. J. Cast Met. Res.*, 26(2013), No. 6, p. 330.
[16] F. Khaleghifar, R. Raiszadeh, and H. Doostmohammadi, Effect of ca on the behavior of double oxide film defects in commercially pure aluminum melt, *Metall. Mater. Trans. B*, 46(2015), No. 2, p. 1044.
[17] E.A. Brandes and G.B. Brook, *Smithells Metals Reference Book*, 7th ed., Butterworth-Heinemann, Oxford, 1998.
[18] B. Feng, J. Weng, B.C. Yang, J.Y. Chen, J.Z. Zhao, L. He, S.K. Qi, and X.D. Zhang, Surface characterization of titanium and adsorption of bovine serum albumin, *Mater. Charact.*, 49(2002), No. 2, p. 129.
[19] J. Pouilleau, D. Devilliers, F. Garrido, S. Durand-Vidal, and E. Mahé, Structure and composition of passive titanium oxide films, *Mater. Sci. Eng. B*, 47(1997), No. 3, p. 235.
[20] A. Shafaei and R. Raiszadeh, Reduced pressure test verification of healing of double oxide film defects in Al–Mg alloys, *Metall. Mater. Trans. B*, 45(2014), No. 6, p. 2486.
[21] M. Aryafar, R. Raiszadeh, and A. Shalbafzadeh, Healing of double oxide film defects in A356 aluminium melt, *J. Mater. Sci.*, 45(2010), No. 11, p. 3041.
[22] D.J. Harach and K.S. Vecchio, Microstructure evolution in metal-intermetallic laminate (MIL) composites synthesized by reactive foil sintering in air, *Metall. Mater. Trans. A*, 32(2001), No. 6, p. 1493.